PULSED MULTI-BAND MIMO FOR UWB SYSTEMS

Craig J. Mitchell, Pedro M. Crespo, and Javier Del Ser

CEIT and TECNUN (University of Navarra)
Paseo Mikeletegi 48, 20009, San Sebastián, Spain
phone: + (34) 943 212 800, fax: + (34) 943 213 076, email:
{cmitchell,pcrespo,jdelser}@ceit.es, web: www.ceit.es

ABSTRACT

This paper provides a solid mathematical framework for pulsed multiband MIMO UWB systems. In this regard a novel multiple-input multiple-output (MIMO) technique for pulse based UWB systems is proposed that exploits multi-band UWB signals for improved performance. Each transmit antenna utilizes a different band for the transmission of the signals. A RAKE receiver is employed that captures energy from sequences transmitted from L transmit antennas at M receive antennas for each of K resolved multipath components. Higher gains in diversity per resolved multipath are achieved with the proposed system than in previously considered zero forced MIMO systems [1] resulting in significant performance enhancement. Diversity gain per path is found to be M for the proposed system as opposed to $M-L+1$ for the zero forcing alternative. Less antennas and/or less combined RAKE paths are therefore required for a certain level of performance. The advantage of utilizing such multiband signaling in a MIMO system are evident from simulated and theoretical results of the system in a simple practical lognormal fading channel developed for the theoretical analysis. Analytical error expressions are also found for the systems presented in this channel model.

1. INTRODUCTION

A lot of academic and commercial interest has been focused on ultra-wideband (UWB) communications. These systems are attractive due to their potential to deliver high data rates over a short distance [2], as well as their ability to occupy the same spectrum as narrow band systems. A few UWB technologies exist, most are either based on OFDM, or on impulse radio (IR-UWB) [3]. A further technique proposed for UWB, termed multiband UWB (MB-UWB) [4], uses impulse radio to transmit pulses in different frequency bands. The available wide bandwidth is split into multiple frequency bands, by using bandlimited pulses and modulating them up with a pseudo-carrier oscillation so as to alter their center frequencies. Higher data rates are possible with better spectral control as bands can be used in parallel. In addition power constraints are imposed on systems which limits the range of transmission, while the data rate is limited by a channel excess delay that may cause inter-symbol interference (ISI) [3].

Diversity is exploited in wireless communications systems to improve performance and combat interference. Spatial diversity is achieved through the use of multiple antennas at transmitter and/or receiver. While this is a well known concept, it still offers large potential for performance improvement in many new wireless technologies. The exploitation of spacial diversity through the use of multiple antennas has been widely researched in narrowband systems. Multiple-input multiple-output (MIMO) systems utilize diversity through multiple antennas at both transmitter and receiver [5].

The application of diversity techniques to IR-UWB systems offers the ability to improve system performance, reduce interference and increase data rate. Most research in this field so far is focused on the performance and capacity of these systems. In [6] a multi-antenna UWB transceiver is proposed for UWB showing improved performance. An IR-UWB MIMO system in a more realistic indoor lognormal fading environment was investigated in [1].

In this paper, MIMO systems employing RAKE type receivers are investigated for practical lognormal fading channels utilizing MB-UWB signaling for improved performance. We exploit the bandwidth separation of MB signals in a MIMO system so as to improve diversity characteristics and performance by increasing data rate and reducing ISI.

2. SYSTEM MODEL

2.1 Transmit Signal

Consider a single input single output (SISO) IR-UWB transmission system utilizing a normalized elementary pulse shape $p_e(t)$. The transmitted BPSK signal emanating from the transmit antenna for such a system can be expressed as

$$x(t)=\sum_{i=0}^{\infty}\sqrt{E_s/N_r}s(\lfloor i/N_r\rfloor)p_e(t-iT_r), \tag{1}$$

where $\lfloor\cdot\rfloor$ denotes the floor, $s(i)$ is the i^{th} transmit symbol (for BPSK $s(i)\in\{-1,1\}$, equiprobable i.i.d random variables), T_r is the pulse repetition period/time, N_r the number of pulses per symbol and E_s the average energy per symbol. We also assume that $p_e(t)$ has a short duration of time support T_p, which is much less than the pulse repetition rate ($T_p \ll T_r$). So as to avoid ISI, T_r is considered to be larger than the channel delay spread. $p_e(t)$ also has a -10dB bandwidth of W_pHz.

2.2 Channel Model

IR-UWB systems are highly frequency selective with received energy scattered over a number of resolvable multipath components [3]. A standard model has been adopted by the IEEE802.15.3a working group exhibiting a clustering of arrival paths. A discrete time decimated version of the channel model can further be found in [7]. This produces a discrete statistical model with K_R multipaths, minimum resolution T_d and impulse response:

$$c(t)=\sum_{k=0}^{K_R-1}h(k)\delta(t-kT_d), \tag{2}$$

where, $h(k)$ is the channel coefficient (fading margin) of the k^{th} resolved multipath component. The minimum multipath resolution is equal to the received pulse duration $T_d=T_p$.

UWB shadowing can be modelled with a lognormally distributed [3] variable. Channel coefficients are assumed $h(k)=\varepsilon(k)\alpha(k)$, where $\varepsilon(k)\in\{-1;1\}$ represents pulse inversions due to reflections and $\alpha(k)$ is a lognormal fading amplitude. The decision variable for multiantenna systems depends on the square of the channel coefficient $\vartheta=h^2(k)$ which also has a lognormal distribution. This variable is defined as $\vartheta=e^{\phi(k)}$, where $\phi(k)$ is a normally distributed random variable with mean μ and variance σ^2,

i.e. $\phi(k) \sim \mathcal{N}(\mu, \sigma^2)$. The probability density function of ϑ is therefore given by [8],

$$p_\vartheta(\vartheta) = \frac{1}{\sqrt{2\pi}\sigma\vartheta} \exp\left[-\frac{(\ln\vartheta - \mu)^2}{2\sigma^2}\right], \quad (3)$$

and the moment generating function (MGF) for ϑ is [8],

$$M_\vartheta(s) \simeq \frac{1}{\sqrt{\pi}} \sum_{n=1}^{N_p} H_{x_n} \exp(e^{(\sqrt{2}\sigma x_n + \mu)/10} s) \quad (4)$$

where x_n and H_{x_n} are the zeros and weight factors of the N_p-order Hermite polynomial [8]. The j^{th} moment of ϑ, is

$$E\left[\vartheta^j\right] = \int_{-\infty}^{\infty} \vartheta^j p_\vartheta(\vartheta) d\vartheta = \exp\left[j\mu + \frac{1}{2}j^2\sigma^2\right]. \quad (5)$$

The average power of path k is assumed $E[\vartheta] = \Omega_0 e^{-\rho k}$, where Ω_0 is the mean energy of the 1st path and ρ is a path decay factor. This is a general lognormal channel model which is easily adapted to more realistic channel profiles with exponential power decay [9] and altering parameters (Ω_0, ρ and σ). The mean μ^k of $\phi(k)$ is $\mu^k = \ln(\Omega_0) - \rho k - (\sigma^2/2)$, given the appropriate values for Ω_0, ρ and σ (from (5)).

2.3 Receive Signal

The resulting received UWB signal when the input to the SISO channel is given by expression (1) is

$$y(t) = \sum_{i=0}^{\infty} \sqrt{\frac{E_s}{N_r}} s(\lfloor \frac{i}{N_r} \rfloor) \sum_{k=1}^{K_R} h(k) p_r(t - \tau_c - iT_r - kT_d) + \varpi(t), \quad (6)$$

where $\varpi(t)$ is a real zero-mean additive white gaussian noise process with power spectral density $N_0/2$ representing independent additive noise and other interference, $h(k)$ is the k^{th} multipath channel coefficient and $p_r(t)$ is the received, and possibly distorted, pulse shape. τ_c represents the channel delay. We will assume that the number of repetition pulses per information symbol is set to 1, i.e, $N_r = 1$, and that $\tau_c = 0$, and that the channel is distortionless, i.e. $p_r(t) = p_e(t)$.

2.4 RAKE Receiver

Due to the large RMS delay spread of the UWB channel, RAKE type receivers are often employed utilizing maximum ratio combining (MRC) [10]. For practicality (complexity) we only consider a subset K ($K \leq K_R$). Each "finger" of the RAKE contains a filter-matched to $p_r(t)$, sampled at each path interval. The output of this is processed on a path by path basis, producing a discrete output $r_i(k)$. The RAKE combines the contributions to form the decision statistics for a symbol-by-symbol detection. Assuming that the receiver has full knowledge of channel coefficients, the MRC decision variable for the i^{th} transmitted symbol becomes,

$$d(i) = \sum_{k=0}^{K-1} h(k) r_i(k). \quad (7)$$

3. MIMO SYSTEMS

3.1 MIMO Channel

Consider a MIMO system with L transmit antennas and M receive antennas. Let $\mathbf{H_k}$ be the $M \times L$ matrix of channel coefficients for the k^{th} multipath component. $h_{m,l}(k)$ represents the k^{th} multipath channel coefficient with respect to the l^{th} transmit to the m^{th} receive antenna.

$$\mathbf{H_k} = \begin{bmatrix} h_{1,1}(k) & h_{1,2}(k) & \cdots & h_{1,L}(k) \\ h_{2,1}(k) & h_{2,2}(k) & \cdots & h_{2,L}(k) \\ \vdots & & \ddots & \vdots \\ h_{M,1}(k) & h_{M,2}(k) & \cdots & h_{M,L}(k) \end{bmatrix}. \quad (8)$$

where the entries $h_{l,m}(k)$ are assumed to be independent lognormal random variables [3].

3.2 Zero Forced MIMO

We now describe the zero forced MIMO system introduced in [1]. The transmit signals for each antenna $x_l(t)$ are as in (1), with $T_p = T_{ZF}$, $W_p = W_{ZF}$ and total transmit energy across all L antennas being LE_s (for simplicity we consider systems with a fixed number of transmit antennas, but this is easily extended to systems with differing numbers of antennas). Assuming perfect synchronization the received vector across the M receive antennas for the kth path is

$$\mathbf{r}(k) = \sqrt{E_s}\mathbf{H_k}\mathbf{s} + \nu(k), \quad (9)$$

where $\mathbf{s} = [s_1(i), s_2(i), \ldots, s_L(i)]^\top$ is the BPSK transmit vector at iT_r, and $\nu(k) = [\varpi_1(k), \varpi_2(k)), \ldots, \varpi_M(t)]^\top$ is a noise vector across the receive antennas, independent of the fading process. The zero forced output is

$$\mathbf{y}(k) = \mathbf{H}_k^+ \mathbf{r}(k) = \sqrt{E_s}\mathbf{s} + \xi(k), \quad (10)$$

where $(\cdot)^+$ denotes the Moore-Penrose pseudoinverse and $\xi(k) = \mathbf{H_k}^+ \nu(k) = [\xi_1(k), \xi_2(k), \ldots, \xi_L(k)]^\top$ denotes the zero forced noise vector with covariance matrix $E[\xi(k)\xi(k)^\top] = \frac{N_0}{2}\mathbf{H}_k^+\mathbf{H}_k^{+\top}$. Under the assumption [1] that $\mathbf{H}_k^\top\mathbf{H}_k$ is a full rank matrix, $\mathbf{H}_k^+\mathbf{H}_k^{+\top}$ reduces to $(\mathbf{H}_k^\top\mathbf{H}_k)^{-1}$. By denoting $\kappa_l(k)^2 \doteq 1/[(\mathbf{H}_k^\top\mathbf{H}_k)^{-1}]_{ll}$, where $[\cdot]_{ll}$ represents the $(l,l)^{th}$ element of the matrix, the MRC decision variable for the transmitted symbol $s_l(i)$ is given by [1]

$$d_l(i) = \sum_{k=0}^{K-1} \kappa_l(k)^2 \left[\sqrt{E_s} s_l(i) + \xi_l(k)\right], \quad (11)$$

yielding an instantaneous SNR

$$\gamma_{s,ZF} = \frac{2E_s}{N_0} \sum_{k=0}^{K-1} \kappa_l(k)^2. \quad (12)$$

From this expression, the per path diversity $\zeta_{ZF}(k)$ obtained for this ZF system will depend on the statistical properties of $\kappa_l(k)^2$. In [1, 11] it was shown that $\kappa_l(k)^2$ can be decomposed as $\kappa_l(k)^2 = \sum_{m=1}^{M-L+1} \hbar_{l,m}(k)^2$, where $(\hbar_{l,1}(k), \ldots, \hbar_{l,M}(k)) = (h_{l,1}(k), \ldots, h_{l,M}(k))\mathbf{U}^\top$, with $\mathbf{U}$ being an appropriate orthonormal matrix. Assuming that $\{h_{l,m}(k)\}_{m=1}^M$ are uncorrelated with covariance matrix $\sigma^2\mathbf{I}$, the random variables $\{\hbar_{l,m}(k)\}_{m=1}^M$ are also uncorrelated with the same covariance matrix[1]. Consequently, the per path diversity is $\zeta_{ZF}(k) = M - L + 1$, i.e. some diversity is used to cancel the interference from the remaining signals.

3.3 Proposed Multi-Band MIMO

In this paper we propose a system that transmits L MB-UWB signals in each of the L transmit antennas. The MB-UWB pulses used for the l^{th} antenna is given by [12]

$$\lambda_l(t) = \sqrt{2} p_e(t) \cos(2\pi f_l t) \quad (13)$$

where $p_e(t)$ is the same elementary pulse shape as in (1), with a different time scale. The pulse has $T_p = T_{MB}$ and $W_p = W_{MB}$. $f_l \in \{f_1, f_2, \ldots, f_L\}$ are the modulating frequencies, and are selected not to overlap (i.e, they are frequency multiplexed). This implies that the distance between f_i and f_j ($i, j \in L$) is at least W_{MB}. To maintain equal spectral efficiency, MB-UWB pulses occupy the same total bandwidth, i.e. $W_{MB} = (1/L)W_{ZF}$, and $T_{MB} = LT_{ZF}$ (achieved by time scaling of $p_e(t)$). This ensures both systems occupy the same bandwidth and have the same transmit energy. For

[1] However they will not be lognormal distributed.

relatively small L, the time support is still less than the repetition time ($T_{MB} \ll T_r$) (by maintaining a low duty cycle and keeping the repetition time T_r constant, the data rates will be equivalent even with the L times increase in pulse width for MB systems). If each transmit antenna uses a different frequency f_l, there is no longer a need for zero forcing. The transmitted signal from the l^{th} antenna is

$$x_l(t) = \sum_{i=-\infty}^{\infty} \sqrt{E_s} s_l(i) \lambda_l(t - iT_r). \tag{14}$$

The received signal, during $iT_r \le t \le (i+1)T_r$, at the m^{th} receive antenna for the k^{th} multipath component is therefore

$$r_m^k(t) = \sum_{l=1}^{L} h_{m,l} \sqrt{E_s} s_l(i) \lambda_l(t - iT_r - kT_d) + \varpi_m(t), \tag{15}$$

where kT_d is the relative delay of the k^{th} multipath and $\varpi_m(t)$ is the real zero-mean additive white gaussian noise process with power spectral density $N_0/2$. Each received antenna requires a bank of L pass-band filters centered at f_i, $i = 1, \ldots, L$ followed by their corresponding demodulators. This recovers the baseband pulses corresponding to symbol $s_l(i)$ at the output of the f_l demodulator, belonging to receive antenna m, i.e. $\sum_{k=0}^{K-1} \sqrt{E_s} s_l(i) h_{m,l}(k) p_e(t - iT_r - kT_d) + n_{m,l}(t)$, where $n_{m,l}(t)$ is the corresponding baseband Gaussian noise. The output of each demodulator enters the RAKE matched filter [9]. This processing done by the RAKE fingers is equivalent to passing such a signal across a bank of K matched filters $g_{m,l}^k(t) = h_{m,l}(k) p_e(T_r - t) \quad k = 0, \ldots, K-1$. Sampling the outputs of these filters at $iT_r + kT_d$, one obtains the set of sufficient statistics for detection

$$\hat{r}_{m,l}^k(i) = h_{m,l}^2(k) \sqrt{E_s} s_l(i) + \xi_{m,l}^k(i) \tag{16}$$

with $\xi_{m,l}^k(i) = n_{m,l} * g_{m,l}(iT_r + kT_d)$, where $*$ denotes convolution. Observe, from the fact that $n_{m,l}(t)$ is a white random process and the multipath components are resolvable, the distribution of the random variables $\xi_{m,l}^k(i)$ conditioned on the channel matrix (i.e., when the entries of (8) are fixed) is Gaussian with zero mean and variances $\frac{N_0}{2} h_{m,l}^2(k)$. Furthermore, they are independent among themselves. The MRC decision variable for estimating transmitted symbol $s_l(i)$ can now be found as the sum of $\hat{r}_{m,l}^k(i)$ over the M receive antennas and K multipath components, that is,

$$d_l(i) = \Upsilon_l \sqrt{E_s} s_l(i) + \mathrm{V}_e, \tag{17}$$

($\Upsilon_l = \sum_{k=0}^{K-1} \sum_{m=1}^{M} h_{m,l}^2(k)$, $\mathrm{V}_e = \sum_{k=0}^{K-1} \sum_{m=1}^{M} \xi_{m,l}^k(i)$)

When conditioned on a fixed channel realization, V_e is the sum of MK independent Gaussian random variables, so V_e itself is Gaussian with zero mean and variance

$$\sigma_{MB}^2 \doteq \mathbb{E}[V_e^2 | \{\mathbf{H}_k\}_{k=0}^{K-1}] = \frac{N_0}{2} \left(\sum_{k=0}^{K-1} \sum_{m=1}^{M} h_{m,l}^2 \right) \tag{18}$$

where $\mathbb{E}[(\cdot)|\{\mathbf{H}_k\}_{k=0}^{K-1}]$ denotes conditional expectation with respect to the MIMO channel. Notice that from expression (17) the instantaneous SNR is easily found to be

$$\gamma_{s,MB} \doteq \frac{2E_s}{N_0} \sum_{k=0}^{K-1} \sum_{m=1}^{M} h_{m,l}^2(k) = \frac{2E_s}{N_0} \Upsilon_l, \tag{19}$$

showing that the per path diversity in the proposed system is given by the statistical properties of $\sum_{m=1}^{M} h_{m,l}^2(k)$, i.e. the sum of M uncorrelated random variables. The path diversity gain is now $\zeta_{MB}(k) = M$, which is an improvement on ZF.

4. PERFORMANCE ANALYSIS

The probability of error $P_{\mathscr{E}}(l,i)$ when estimating symbol $s_l(i)$ based on the MRC observation (17) is

$$P_{\mathscr{E}}(l,i) = \mathbb{E}\left[P_{\mathscr{E}}(l,i|\{\mathbf{H}_k\}_{k=0}^{K-1}) \right] \tag{20}$$

where expectation $\mathbb{E}$ is over all the channel coefficients and $P_{\mathscr{E}}(l,i|(\{\mathbf{H}_k\}_{k=0}^{K-1}))$ is the probability of decision error for symbol $s_l(i)$ conditioned on a fixed channel realization. From (17), $P_{\mathscr{E}}(l,i|\{\mathbf{H}_k\}_{k=0}^{K-1})$ is given by the symbol error expression of a 2-PAM (BPSK) constellation, i.e.,

$$P_{\mathscr{E}}(l,i|\{\mathbf{H}_k\}_{k=0}^{K-1}) = Q\left(\sqrt{\frac{D_{l,i}^2(\{\mathbf{H}_k\}_{k=0}^{K-1})}{4\sigma_{MB}^2}} \right), \tag{21}$$

where $D_{l,i}(\{\mathbf{H}_k\}_{k=0}^{K-1})$ is the euclidian distance between the received constellation symbols in $d_l(i)$, i.e., $\pm\Upsilon_l\sqrt{E_s}$ (for a given a realization of the channel coefficients), σ_{MB}^2 is the conditioned variance of the noise V_e given in expression (18), and $Q(x) = (1/\sqrt{2\pi}) \int_x^{\infty} e^{-u^2/2} du$ is the standard Q-function [9]. Therefore, expression (20) reduces to

$$P_{\mathscr{E}}(l,i) = \mathbb{E}\left[P_{\mathscr{E}}(l,i|\{\mathbf{H}_k\}_{k=0}^{K-1}) \right] = \mathbb{E}\left[Q\left(\sqrt{\frac{2E_s}{N_0}} \Upsilon_l \right) \right] \tag{22}$$

where $\mathbb{E}$ denotes expectation with respect to the random variable Υ. Notice that from the stationarity of the model $P_{\mathscr{E}}(l,i)$ does not depend on i. Expression (22) becomes

$$P_{\mathscr{E}}(l) = \int_{-\infty}^{\infty} Q\left(\sqrt{\frac{2E_s}{N_0}} \upsilon \right) p_{\Upsilon_l}(\upsilon) d\upsilon \tag{23}$$

where $p_{\Upsilon_l}(\upsilon)$ is the probability density function of Υ_l. Recall, that Υ_l is the sum of lognormal random variables $h_{m,l}^2(k)$. To compute this integral we use the following definition for the Q-function $\mathscr{Q}(x) = \frac{1}{\pi} \int_0^{\frac{\pi}{2}} \exp\left(-\frac{x^2}{2\sin^2\theta} \right) d\theta$ [8] along with the MGF (4) in (22) giving

$$P_{\mathscr{E}}(l) = \frac{1}{\pi} \int_0^{\frac{\pi}{2}} M_{\Upsilon_l}\left(-\frac{\frac{E_s}{N_0}}{\sin^2\phi} \right) d\phi, \tag{24}$$

To proceed we need the MGF of Υ_l, which is the sum of independent lognormal random variables $h_{m,l}^2(k)$. $M_{\Upsilon}(s)$ is given by the product of the MGF's of $h_{m,l}^2(k)$,i.e.

$$M_{\Upsilon_l}(s) = \prod_{k=0}^{K-1} \prod_{m=1}^{M} M_{h_{m,l}^2(k)}(s) \tag{25}$$

where the $M_{h_{m,l}^2(k)}(s)$ are the MGF's (4) with fading statistics, $\mu_{m,l}^k$ and $\sigma_{m,l}^k$. Notice that realistic independent selection of fading statistics for each arrival path is possible.

5. NUMERICAL RESULTS

In this section we evaluate the proposed system with some numerical examples. BPSK with a RAKE receiver (fingers situated at each of the K resolved arrival paths) is assumed for all simulations. In general $M \ge L \ge 1$ and $K \ge 1$. The receiver is assumed to have perfect knowledge of all channel coefficients. Detection of the symbols is carried out as in (7), (11) and (17). We further limit ourselves to studying systems that contain 3 transmit antennas. Lognormal fading envelopes are produced with $\alpha(k) = e^{\varphi(k)}$, where $\varphi(k) \sim \mathscr{N}(\mu_\varphi, \sigma_\varphi^2)$. The standard deviation σ_φ of $\alpha(k)$ is set to 3dB as in [7].

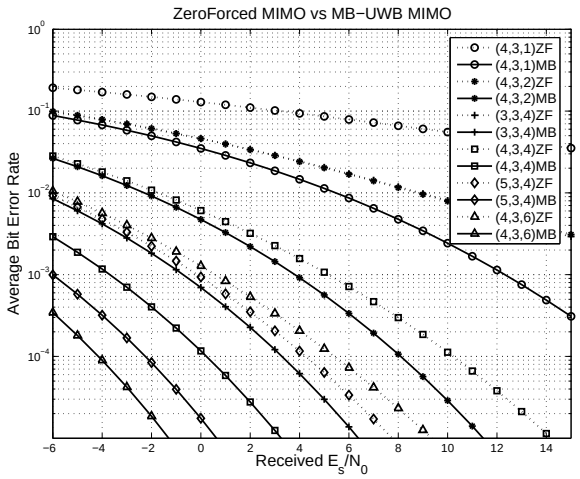

Figure 1: Comparison of the zero forced MIMO (ZF) and Proposed MB-UWB MIMO (MB) systems with different (M,L,K).

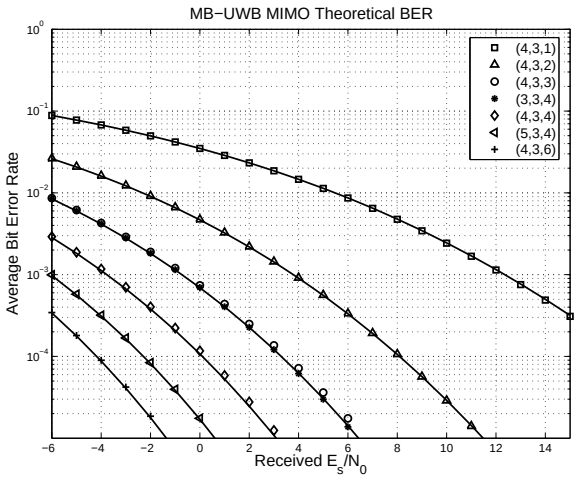

Figure 2: Comparison of simulated (shown with markers) and theoretical (shown with solid lines) BER curves for the proposed system

5.1 Equal Power Paths

To demonstrate the advantages of the proposed multiband system over the zero forcing system we start by assuming that the average power of the strongest path is approximately equal to the average power of the weakest combined path. With a small number of paths the power decay between them can be assumed to be very small. We initially assume that all K paths have normalized equal power, i.e. $\Omega_0 = 1$ and $\rho = 0$.

Recall that the spatial diversity order in a zero forcing algorithm is $M - L + 1$, while in the MB-UWB scheme it remains M. As all the arrival paths have equal average normalized power, the total diversity is $\eta = K\zeta$.

5.1.1 Performance Comparison

Figure 1 compares simulated bit error rate curves with different (M,L,K), for both MB-UWB and Zero Forced systems. In the absence of additional channel coding, the MB-UWB MIMO system shows significant advantage over the zero forced system using the same parameters (antennas and RAKE paths) as we are not losing any diversity for separating the signals. One can view the proposed MIMO system as a parallel transmission of the L symbols with M spatial diversity branches. Both systems show improved performance as the number of paths combined increases. This increase in RAKE order does however increase the hardware complexity of the system. It is noticed that comparing the following pairs of zero forced systems and proposed MB-UWB systems show some similarities, especially at low values of E_s/N_0. E.g. $(4,3,2)ZF \leftrightarrow (4,3,1)MB$, $(4,3,4)ZF \leftrightarrow (4,3,2)MB$ and $(4,3,6)ZF, (5,3,4)ZF \leftrightarrow (3,3,4)MB$. Calculating ζ for each, we see that this is due to them having equal diversity gains in this practical channel model. These curves are not exactly the same and diverge at higher E_s/N_0 values due to the instantaneous SNR for the MB-UWB system (19) depending on the sum of the square of lognormal variables, while that for the ZF algorithm (12) depends on non lognormal random variables. This causes the BER curves to diverge as the SNR value increases with the MB-UWB system performing better.

Each additional receive antenna improves the diversity order obtained in both systems, however, the diversity achieved for the same (M,L,K) is significantly higher in the proposed MB system. The increased diversity gain in the MB-UWB system requires less paths K to combine or less receive antennas M to obtain the same diversity as its ZF counterpart. It is clearly seen that with equal noise in the systems, the proposed MB-MIMO systems outperform their ZF counterparts by a large margin when they utilize the same (M,L,K).

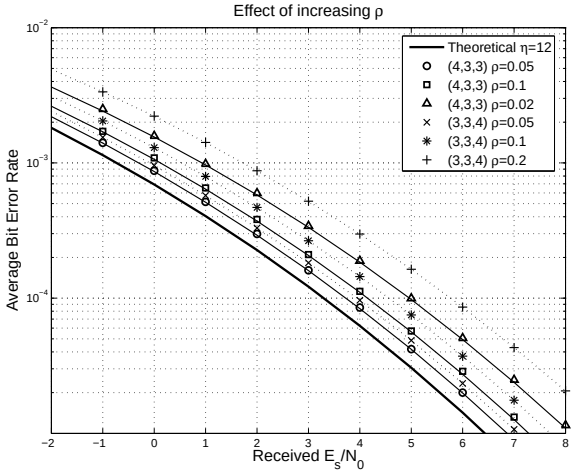

Figure 3: The effect of increasing ρ on the BER of the Multiband (MB) MIMO System. Simulated values shown with markers and theoretical values for $(4,3,3)$ and $(3,3,4)$ systems shown with solid and dashed lines respectively

5.1.2 Theoretical Performance

Figure 2 shows a comparison of the simulated results (shown with markers), and the accuracy of theoretical error values (shown with solid lines) calculated using equation (25).

5.2 Decaying Path Profile

We now consider the case where an average power decay in the path profile exists, i.e. $\rho \neq 0$. Figure 3 shows the effect of a decay in the path profile, i.e. $\rho \neq 0$. Plots are shown for (M,L,K) equal to $(3,3,4)$ and $(4,3,3)$ respectively. These values are chosen as in the equal power case - they both have the same diversity gain $\eta = 12$ and therefore the same performance when $\rho = 0$. When there is a path decay ($\rho \neq 0$), it is seen that the $(4,3,3)$ system performs better than the $(3,3,4)$ one. As ρ increases the difference in performance also increases. This is because the system that combines more paths has less average power per path due to the decay, while the system with more antennas has more average energy per branch. Temporal diversity is less efficient than the spatial diversity due to the path decay. Once again theoretical values (from (25)) and simulated values for the system with the path decay show very good correlation. Similar performance improvements are observed when the system is evaluated on the IEEE 802.15.3a (CM1) channel model [7]. For the purpose of fair comparison between the two systems (ZF and

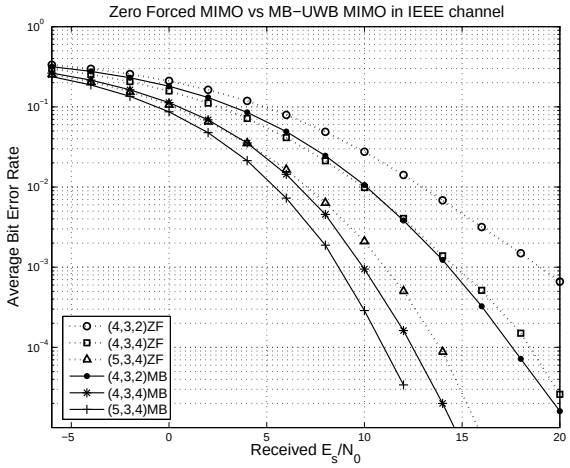

Figure 4: The BER performance of the Zero Forced (ZF) and Multiband (MB) MIMO System on the IEEE 802.15.3a CM1 with different parameters

MB) the channel model is decimated (according [7] section 3.3.3.). The zero forced MIMO system is assumed to have a resolution of 0.167ns and the proposed MB-UWB-MIMO system has a sample time of 0.501ns (due to the L times increase in pulse width). The result is that the 2 systems see the same channel allowing for accurate comparison.

Figure 4 shows the performance of the two systems with this model. It can be clearly seen that the proposed system once again outperforms the zero forced alternative with the same parameters (antennas and RAKE fingers). It is also seen that the zero forced $(4,3,4)$ and the proposed multiband $(4,3,2)$ systems have similar performance at lower E_s/N_0 values and then diverge as this value improves. Again, this is due to them having the same diversity orders and the fact that the typical values of ρ for this realistic channel are very low resulting in the average energy in the arrival paths being almost the same (ZF system sees 4 paths, MB system sees 2). This validates the mathematical framework presented in the paper before as a good method for measuring performance of the proposed systems. At higher E_s/N_0 values it can be seen the the proposed multiband system performs better with its decision based on the lognormally distributed variables. Analytical error results can be obtained for this channel model in the exact same way as before if values for Ω_0, ρ, μ and σ are known for each arrival path.

6. CONCLUSION

A novel multiband based MIMO system has been proposed for use in IR-UWB systems. Previously considered zero forced MIMO systems for IR-UWB are seen to have poor performance, which can be easily surpassed with the system proposed here. Analysis of the error performance of the proposed system over a practical lognormal channel has also been provided, which agrees very well with simulated results.

Both ZF and MB-UWB receivers operate on a path by path basis capturing resolvable components in a RAKE type receiver and allowing for both temporal and spatial diversity gains. The use of the multiple frequency bands allows one to achieve greater diversity gain. The diversity gain is seen to drop to $M-L+1$ for the conventional ZF MIMO, but remains at M in the proposed system. While there is a small cost in complexity due to the mulitband requirement at both transmitter and receiver, the proposed system requires less combined RAKE paths, which is important when there is a power decay profile as paths contain less energy (temporal diversity is less efficient than spatial diversity). The proposed system also requires less antennas to achieve the same diversity gain, which is advantageous as there may be a space constraint on smaller devices. The use of the multiband approach also allows one to control the spectrum of the transmitted signals as individual bands can be suppressed by selecting appropriate f_l's.

Acknowledgments

This work has been supported by the *Ministerio de Educación y Ciencia* of Spain and FEDER funds from the European Union, under grant number TEC2004-06451-C05-04/TCM, as well as by Basque Government Ministry of Industry under TEC-MAR (IBA/PI2004-3) and INFOSETEC (S-PE06CE10) research projects.

REFERENCES

[1] H. Liu, R. C. Qiu, and Z. Tian, "Error performance of pulse-based ultra-wideband mimo systems over indoor wireless channels," *IEEE Transactions on Wireless Communications*, November 2005.

[2] S. Roy, J. R. Foerster, V. S. Somayazulu, and D. G. Leeper, "Ultrawideband radio design: The promise of high-speed, short-range wireless connectivity," *Proceedings of the IEEE*, vol. 92, no. 2, pp. 295–311, February 2004.

[3] A. F. Molisch and J. R. Foerster, "Channel models for ultrawideband personal area networks," *IEEE Wireless Communications Magazine*, pp. 14–21, December 2003.

[4] X. Lou, L. Yang, and G. B. Giannakis, "Designing optimal pulse-shapers for ultra-wideband radios," *Journal of Communications and Networks JCN*, vol. 5, no. 4, pp. 344–353, December 2003.

[5] M. Weisenhorn and W. Hirt, "Performance of binary antipodal signaling over the indoor uwb mimo channel," in *International Conference on Communications. ICC '03.* Anchorage, Alaska: IEEE, May 2003, pp. 2872–2878.

[6] E. Baccarelli, M. Biagi, C. Pelizzoni, and P. Bellotti, "A novel multi-antenna impulse radio UWB transceiver for broadband high-throughput 4G WLANs," *IEEE Communications Letters*, vol. 8, no. 7, pp. 419–421, July 2004.

[7] J. Foerster, "Channel model sub-comittee report final," IEEE P802.15 Working group for WPAN, Tech. Rep. IEEE 802.15-02/490r1-SG3a, February 2003.

[8] M. K. Simon and M.-S. Alouini, *Digital Communications over Fading Channels*, J. G. Proakis, Ed. John Wiley and Sons,Ltd, 2000.

[9] J. G. Proakis, *Digital Communications*, 4th ed. New York, NY: Mc-Graw-Hill, 2000.

[10] M. Win, G. Chriskos, and N. Sollenberger, "Performance of rake reception in dense multipath channels: Implications of spreading bandwidth and selection diversity order," *IEEE Journal on Selected Areas in Communications*, vol. 18, no. 2, pp. 1516–1525, August 2000.

[11] J. H. Winters, J. Salz, and R. D. Gitlin, "The impact of antenna diversity on the capacity of wireless communications systems," *IEEE Transactions on Communications*, vol. 42, no. 2/3/4, pp. 1740–1751, February/March/April 1994.

[12] M. Ghavami, L. B. Michael, and R. Khono, *Ultra Wideband Signals and Systems in Communication Engineering*. John Wiley and Sons,Ltd, 2004.